Materials Letters 68 (2012) 463–465

Contents lists available at SciVerse ScienceDirect

Materials Letters

journal homepage: www.elsevier.com/locate/matlet

Formation of nano-crystalline Si quantum dots in ZnO thin-films using a ZnO/Si multilayer structure

Kuang-Yang Kuo, Shu-Wei Hsu, Wen-Ling Chuang, Po-Tsung Lee *

Department of Photonics & Institute of Electro-Optical Engineering, National Chiao Tung University, Hsinchu 30010, Taiwan

ARTICLE INFO

Article history:
Received 16 September 2011
Accepted 4 November 2011
Available online 10 November 2011

Keywords:
Si quantum dot
ZnO
Sputtering
Thin-films

ABSTRACT

In this study, we propose to fabricate ZnO thin-films with nano-crystalline Si (nc-Si) quantum dots (QDs) embedded using a ZnO/Si multilayer structure by radio-frequency (RF) magnetron sputtering method. Our results show that a high Si sputtering power (P_{Si}) can assist the formation of self-aggregated Si nano-clusters during deposition, which is helpful for the crystallization of nc-Si QDs and ZnO matrix during annealing. Great crystallinity and highly uniform size of nc-Si QDs are obtained for P_{Si} of 110 W. We experimentally demonstrate the formation of nc-Si QDs embedded in crystalline ZnO thin-films, which has a great potential for various electro-optical device applications.

© 2011 Elsevier B.V. All rights reserved.

1. Introduction

Recently, the nano-crystalline Si (nc-Si) quantum dots (QDs) embedded in Si-based dielectric materials like SiO_2 and Si_3N_4 had been extensively studied and integrated into various electro-optical devices such as light-emitting diodes (LEDs) [1] and photovoltaics (PVs) [2]. LEDs with multi-color light emission properties using nc-Si QDs had been successfully developed by Lai BH et al. [1], and Cho EC et al. had integrated nc-Si QDs into PVs for the third-generation PVs development [2]. Therefore, the nc-Si QD indeed has a great potential for a variety of electro-optical applications. In this report, we propose to fabricate nc-Si QDs embedded in ZnO thin-films because ZnO has many suitable features such as wide bandgap, high transparency, and tunable conductivity. In addition, ZnO is a well-known semiconductor material and its conductivity can be easily tuned to provide desirable electrical properties [3]. Therefore, ZnO can serve as the matrix material for nc-Si QDs for bandgap engineering and efficiently decrease the light absorption loss from matrix material to enhance the performance of electro-optical devices. Besides, ZnO is also a promising material for spintronic applications because of its ferromagnetic behavior, which depends on the nano-structured characteristics of ZnO [4]. Hence, the optical and magnetic properties originating from the interaction of nc-Si QDs with ZnO matrix could also be an interesting and meaningful research topic. Undoubtedly, there are many advantages to embed nc-Si QDs in ZnO thin-films, and it's important to demonstrate the possibility on the realization of nc-Si QDs embedded ZnO thin-films. In this study, we fabricate the nc-Si QDs in ZnO thin-films using a ZnO/Si multilayer (ML) deposition structure and a post-annealing process, and investigate the formation mechanism and nano-structured properties.

2. Experiment

The ZnO/Si ML thin-films with 24-bilayers are deposited on Si(100) wafers by radio-frequency (RF) magnetron sputtering method. The sputtering power of Si (P_{Si}) is varied from 25 (S25) to 110 W (S110) while that of ZnO is fixed at 75 W. The effective thicknesses of each ZnO and Si layers are fixed at 5 and 3 nm, respectively. After deposition, the ZnO/Si ML thin-films are annealed by a rapid thermal annealing (RTA) process at 1000 °C for 50 s under N_2 flow since an annealing temperature higher than 900 °C is generally needed for the nc-Si QDs formation [5]. The Raman spectra are measured using a 488 nm diode-pumped solid-state laser (Horiba LabRam HR). The X-ray diffraction (XRD) patterns are examined by a Bede-D1 X-ray diffractometer with Cu K_{α} radiation. The surface morphologies are analyzed by a Digital Instrument D3100 atomic force microscope (AFM). The high-resolution transmission electron microscope (HRTEM) images are obtained by a JEOL JEM-2010F transmission electron microscope.

3. Results and discussion

To confirm the nc-Si QDs formation, Raman measurement, a well-known and credible technique for examining the nc-Si properties [6,7], is performed. Fig. 1(a) shows the Raman spectra of the annealed ZnO/Si ML thin-films under different P_{Si} and its inset shows the curve-fitting result of Raman spectrum for sample S110. The fitting curve, which is decomposed into four components with peaks located at 436.1, 480.0, 508.3, and 519.7 cm^{-1}, shows an excellent match with

* Corresponding author. Tel.: +886 3 5712121x31306; fax: +886 3 5735601.
E-mail address: potsung@mail.NCTU.edu.tw (P.-T. Lee).

0167-577X/$ – see front matter © 2011 Elsevier B.V. All rights reserved.
doi:10.1016/j.matlet.2011.11.022

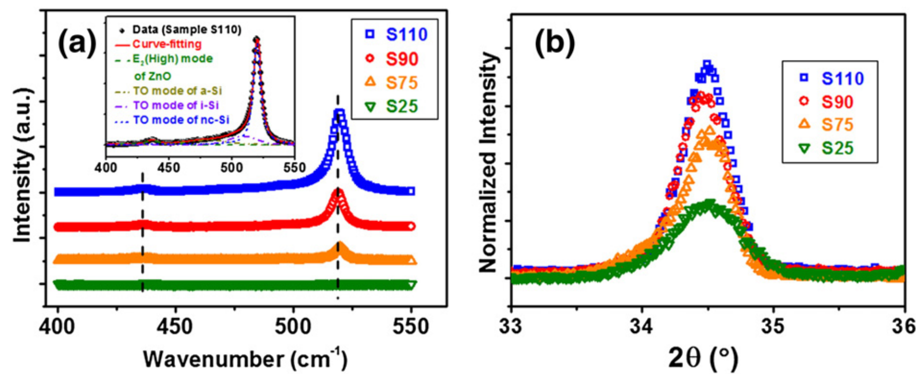

Fig. 1. (a) Raman spectra and (b) XRD patterns of the annealed ZnO/Si ML thin-films under different P_{Si}. Inset of (a) shows the curve-fitting result of Raman spectrum for sample S110.

the measured data. The peaks at 480.0, 508.3, and 519.7 cm^{-1} are usually observed in the nc-Si QD, and they are contributed from the transverse-optical (TO) modes of Si–Si vibrations in the amorphous (a-Si), intermediate (i-Si), and nc-Si phases of Si, where the i-Si phase is caused by grain boundaries or smaller crystallites [6]. The FWHM of nc-Si phase is 7.4 cm^{-1}, corresponding to nc-Si size about 4 nm [7]. The peak at 436.1 cm^{-1} comes from the E_2(high) mode of ZnO. The lower peak position than 439 cm^{-1} of bulk ZnO is attributed to the presence of intrinsic defects in the ZnO nano-clusters [8]. The peak near 520 cm^{-1} is not observed in sample S25 and significantly increases from samples S75 to S110. Besides, sample S110 shows not only the largest Si crystalline intensity but also a great Si crystal volume fraction (f_c) of 88%, where f_c is estimated from the sum of the integrated intensities of nc-Si and i-Si phases divided by the total sum of the integrated intensities of nc-Si, i-Si, and a-Si phases [9].

The crystalline property of ZnO matrix has strong influences on the optical and electrical properties of ZnO thin-films [3]. Fig. 1(b) shows the XRD patterns of the annealed ZnO/Si ML thin-films under different P_{Si} for the examination of the c-axis (0002) preferred orientation of ZnO matrix. The ZnO/Si ML thin-films exhibit a narrower FWHM and higher intensity when increasing P_{Si}. This means a better crystallization of ZnO matrix can be obtained with a higher P_{Si}. Hence, the results in Raman spectra and XRD patterns indicate that a high enough P_{Si} is necessary for the formation of nc-Si embedded in ZnO matrix and the increased P_{Si} can improve the crystalline properties of both nc-Si and ZnO matrix.

In order to understand the formation mechanism, we analyze the AFM images of the ZnO single-layer with a 5 nm thickness and the ZnO/Si single-bilayer under different P_{Si} after deposition, as shown in Fig. 2. Significant variations on the surface morphologies are observed. The AFM image of sample S25 shows a smaller root-mean-square (RMS) surface roughness than that of the ZnO single-layer, and the deposited Si layer can be seen as a thin layer-like. However, the AFM images of samples S75, S90, and S110 show larger RMS surface roughnesses than that of ZnO single-layer and clear formation of a-Si nano-clusters. Moreover, the RMS surface roughness increases with increasing P_{Si} and the density of nano-clusters in samples S90 and S110 can be estimated to be 3.1×10^{10} and 1.9×10^{10} cm^{-2}. The similar results are also obtained in the ZnO/Si double-bilayers. Since an a-Si nano-film needs a higher crystallization temperature of 1100 °C than that for a-Si nano-clusters [10], the nc-Si is hard to efficiently form in sample S25 during annealing. The more obvious formation of a-Si nano-clusters with increasing P_{Si} indicates that a higher P_{Si} can remarkably assist the sputtered Si atoms gaining more kinetic energy to self-aggregate as a-Si nano-clusters during deposition. Therefore, nc-Si QDs can be formed more easily during annealing. This observation is in good agreement with the Raman results. The peak intensity of the nc-Si is greatly enhanced with increasing P_{Si}. Furthermore, because each ZnO thin-layer is separated by the a-Si thin-layer in sample S25, the crystallization of ZnO matrix is impeded during annealing. Hence, a lower quality of ZnO crystallization is obtained in sample S25.

The as-deposited and after-annealing cross-sectional HRTEM images of sample S110 are shown in Fig. 3. In Fig. 3(a) and (b), we can observe the obvious ML structure with a slightly rough morphology and the formation of a-Si nano-clusters with a size distribution of 3–5 nm separated by ZnO thin-layers after deposition. The slightly rough morphology is different from the ML structures using Si-based dielectric materials as matrix [11]. This result is reasonable since ZnO is easy to crystallize during deposition [3]. We can adjust the morphology of each ZnO thin-layer by tuning the ZnO sputtering power or the working pressure during deposition. The observed size distribution of a-Si nano-clusters is highly consistent with the examined height of a-Si nano-clusters in AFM image and the estimated size of nc-Si about 4 nm in Raman spectrum for sample S110, and such size is suitable for various electro-optical devices using the quantum-confinement effect. From Fig. 3(c), the ML structure can still be clearly seen after annealing and a high-density of nano-crystalline clusters with a size distribution of 2–6 nm can be observed from the zoom-in HRTEM image shown in Fig. 3(d). Combined with the Raman and

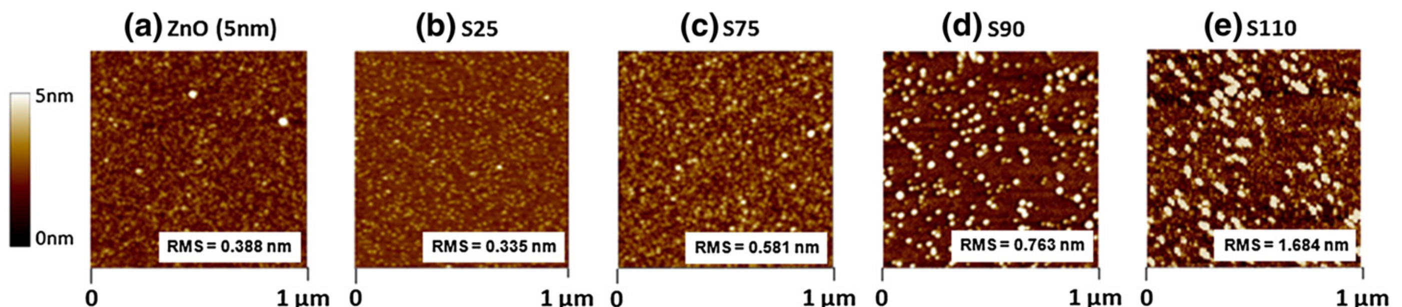

Fig. 2. AFM images of (a) the ZnO single-layer with a 5 nm thickness and the ZnO/Si single-bilayer thin-films under (b) 25, (c) 75, (d) 90, and (e) 110 W of P_{Si} after deposition.

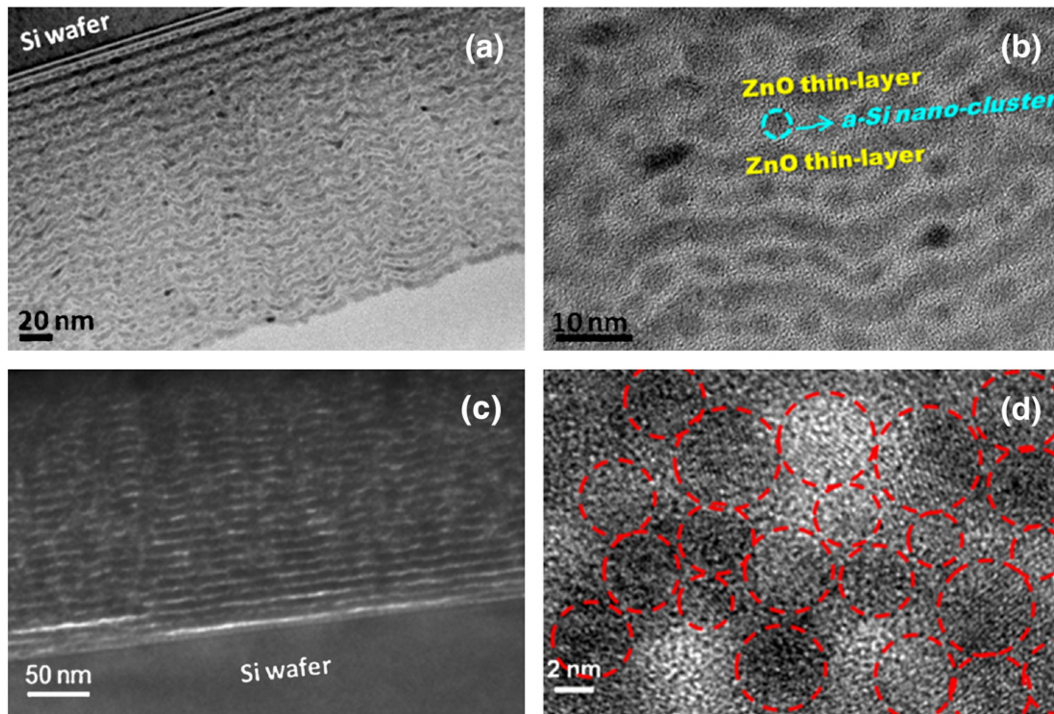

Fig. 3. The overall and zoom-in cross-sectional HRTEM images of the ZnO/Si ML thin-film. (a) and (b) are as-deposited, and (c) and (d) are after annealing for sample S110.

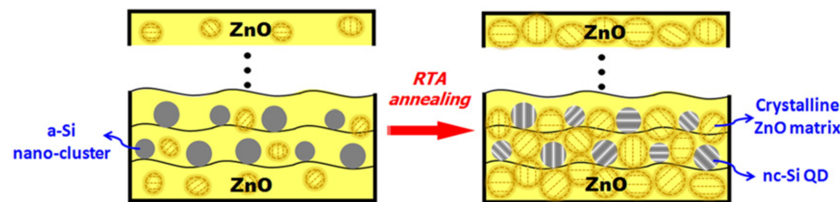

Fig. 4. Illustration of the formation of nc-Si QDs embedded in the crystalline ZnO matrix with a high enough P_{Si} in a ZnO/Si ML structure.

XRD results, these nano-crystalline clusters are the nc-Si QDs embedded in crystalline ZnO matrix. Therefore, we can conclude that a high P_{Si} can assist the formation of self-aggregated a-Si nano-clusters on ZnO layers during deposition, and such result is advantageous to form the nc-Si QDs embedded in crystalline ZnO matrix during annealing, as illustrated in Fig. 4. Thus, we demonstrate that the good crystallization of nc-Si QDs and ZnO matrix can be simultaneously achieved with a high enough P_{Si} for the nc-Si QDs embedded ZnO thin-films.

4. Conclusion

In summary, we propose to fabricate nc-Si QDs in ZnO thin-films and successfully demonstrate their formation. The sample with P_{Si} of 110 W shows a large f_c of 88% and a highly uniform size about 4 nm of nc-Si QDs. Our results indicate that an obvious self-aggregation of the sputtered Si atoms as nano-clusters with a high enough P_{Si} during deposition is essential and helpful for the nc-Si QDs formation and the better crystallization of ZnO matrix during annealing. Therefore, we demonstrate the feasibility of fabricating nc-Si QDs embedded in crystalline ZnO thin-films. We believe this proposed structure has a great potential for the applications in various electro-optical or spintronic devices.

Acknowledgments

This work is supported by Taiwan's National Science Council (NSC) under contract number NSC-100-2120-M-009-005. The authors would like to thank the help from Center for Nano Science and Technology (CNST) of National Chiao Tung University and National Nano Device Laboratories (NDL) in Taiwan.

References

[1] Lai BH, Cheng CH, Lin GR. IEEE J Quantum Electron 2011;47:698.
[2] Cho EC, Park S, Hao X, Song D, Conibeer G, Park SC, et al. Nanotechnology 2008;19: 245201.
[3] Özgür Ü, Alivov YI, Liu C, Teke A, Reshnikov MA, Dogan S, et al. J Appl Phys 2005;98:041301.
[4] Straumal BB, Protasova SG, Mazilkin AA, Myatiev AA, Straumal PB, Schütz G, et al. J Appl Phys 2010;108:073923.
[5] Mirabella S, Agosta R, Franzò G, Crupi I, Miritello M, Savio RL, et al. J Appl Phys 2009;106:103505.
[6] Cheng Q, Tam E, Xu S, Ostrikov K. Nanoscale 2010;2:594.
[7] Faraci G, Gibilisco S, Russo P, Pennisi AR, Compagnini G, Battiato S, et al. Eur Phys J B 2005;46:457.
[8] Alim KA, Fonoberov VA, Balandin AA. Appl Phys Lett 2005;86:053103.
[9] Cheng QJ, Xu S, Ostrikov K. Nanotechnology 2009;20:215606.
[10] Zacharias M, Blasing J, Veit P, Tsybeskov L, Hirschman K, Fauchet PM. Appl Phys Lett 1999;74:2614.
[11] Cho EC, Green MA, Conibeer G, Song D, Cho YH, Scardera G, et al. Adv Opt Electron 2007;2007:69578.